



RESEARCH REPORT

PERMANENT WAVE STRUCTURES on an OPEN TWO LAYER FLUID

by
P. J. BRYANT

No. 1

November 1976

Department of Mathematics

University of Canterbury
Christchurch
New Zealand

PERMANENT WAVE STRUCTURES ON AN
OPEN TWO LAYER FLUID

By P.J. Bryant

There is a significant nonlinear interaction between fast free surface waves and slow interface waves when the group velocity of the free surface waves is the same as the phase velocity of the interface waves. This interaction leads to permanent wave structures consisting of a wave group of permanent envelope on the free surface and a wave of permanent shape on the interface. A theory is developed for periodic permanent wave structures of this type, from which solutions are found numerically. The theory includes all significant quadratic nonlinear interactions between free surface harmonics and interface harmonics, as well as between the interface harmonics themselves. It is found that there is a sequence of forms of differing free surface group structure.

1. Introduction.

Two uniform layers of fluid with densities of similar magnitude and a free upper surface have two modes of gravity wave propagation, a fast free surface wave mode and a slow interface wave mode. When both wave modes are present, a nonlinear interaction occurs between them. Benney [1] has shown that the nonlinear interaction is resonant when the group velocity of the fast free surface wave mode equals the phase velocity of the slow interface wave mode. This property leads to permanent wave structures in which a wave group of permanent envelope on the free surface is coupled with and moves with the same velocity as a permanent wave on the interface.

The interaction between surface waves and internal waves has been studied previously in terms of the response of the surface waves to the velocity field caused at the surface by the internal waves [2, 3, 4]. The concept of radiation stress was used to determine the behaviour of a surface wave under the influence of a prescribed internal wave. This method is unsatisfactory for the present problem because the shape of the internal wave, as well as the shape of the surface wave, are unknown quantities. It was found in these investigations that maximum interaction occurs when the phase velocity of the internal wave and the group velocity of the surface wave are matched.

The approach used here is to assume that the wave propagation is unidirectional and is spatially periodic. The surface and interface waves may then be represented by Fourier series whose coefficients have a slow time dependence. Equations are found for the time rate of change of each Fourier amplitude in terms of all significant quadratic interactions between all Fourier amplitudes. Solutions describing permanent wave structures are found from these equations. In the limit as the fundamental wavelength becomes large compared with the depth, the Fourier series tend towards Fourier transforms of a solitary permanent wave structure.

The properties of long waves on a shallow uniform *single* layer fluid are dominated by the near-resonant nature of the interactions between wave harmonics [5, 6]. If k and ℓ denote the wavenumbers of two long wave harmonics propagating in the same direction with frequencies ω_k, ω_ℓ , then

$$\omega_k + \omega_\ell - \omega_{k+\ell} = O(\mu^2), \quad (1.1)$$

where μ is a measure of the ratio of fluid depth to wavelength. For waves long compared with the depth, this near-resonant interaction causes the $k+\ell$ harmonic to grow to an amplitude comparable with the amplitudes of the k and ℓ harmonics separately. A long periodic wave therefore contains a large number of harmonics, whose amplitudes decrease with increasing wavenumber because their interactions move further from resonance. The long periodic waves of permanent form are approximated by cnoidal waves, tending towards solitary waves as the separation between consecutive crests increases.

The same general properties are valid for single mode permanent waves in a two layer fluid. Peters & Stoker [7] have shown that there exist fast free surface permanent waves and slow interface permanent waves. The near-resonant condition (equation 1.1) then applies respectively either to the frequencies of the fast free surface wave harmonics alone, or to the frequencies of the slow interface wave harmonics alone.

When both wave modes are present, significant near-resonant interactions occur between free surface and interface wave harmonics in the neighbourhood of wavenumbers $\Delta k, k, k + \Delta k$ ($\Delta k \ll k$) for which

$$(\omega_{k+\Delta k})_{\text{free surface}} - (\omega_k)_{\text{free surface}} - (\omega_{\Delta k})_{\text{interface}} = 0. \quad (1.2)$$

This near-resonant interaction takes two forms. It may describe an interface wave harmonic of small wavenumber interacting with a free surface wave harmonic of large wavenumber to modify another free surface wave harmonic of large wavenumber. This is the nonlinear interaction that generates free surface wavenumbers over a broad waveband to form a wave group. It may also describe two free surface waves harmonics of large wavenumber

interacting to modify an interface wave harmonic of small wavenumber. This is the nonlinear interaction that generates interface waves in the presence of a group of free surface waves. It will be seen later (§§ 5, 6) that equation (1.2) is modified by the horizontal velocity caused at the free surface by the wave on the interface, but that this modification does not alter the validity of the above arguments.

2. Governing equations.

The two layer fluid consists of a lower layer of mean depth h_1 and density ρ_1 on a horizontal bottom, and an upper layer of mean depth h_2 and density ρ_2 with a free upper surface. Attention is confined to fluids for which the density difference $\rho_1 - \rho_2$ is small compared with ρ_1 and ρ_2 . The fundamental wavelength is denoted by $2\pi\ell$, and a, b are measure of free surface and interface wave amplitudes respectively, to be defined more precisely later. The horizontal and vertical coordinates x, y are non-dimensional, being measured in units of $h_1 + h_2$, and the origin of y is on the mean interface. The time t is non-dimensional in units of $((h_1 + h_2)/g)^{1/2}$, where g is gravity. Interface displacement, η , and free surface displacement ξ , are measured in units of b , and both velocity potentials ϕ_1, ϕ_2 in units of $(g(h_1 + h_2)^3)^{1/2}$. The principal small parameter is $\epsilon = b/(h_1 + h_2) \ll 1$, and other non-dimensional parameters are $\epsilon' = a/(h_1 + h_2) \ll 1$, $\mu = (h_1 + h_2)/\ell$, $\rho = \rho_1/\rho_2$, $h = h_1/(h_1 + h_2)$.

The governing equations are then

$$\phi_{1xx} + \phi_{1yy} = 0 \quad , \quad -h < y < 0 \quad , \quad (2.1a)$$

$$\phi_{2xx} + \phi_{2yy} = 0 \quad , \quad 0 < y < 1 - h \quad (2.1b)$$

$$\phi_{1y} = 0 \text{ on } y = -h, \quad (2.1c)$$

$$\phi_{1y} - \eta_t - \epsilon(\eta\phi_{1x})_x = 0(\epsilon^2) \text{ on } y = 0, \quad (2.1d)$$

$$\phi_{2y} - \eta_t - \epsilon(\eta\phi_{2x})_x = 0(\epsilon^2) \text{ on } y = 0, \quad (2.1e)$$

$$\rho\phi_{1t} - \phi_{2t} + (\rho - 1)\eta + \epsilon\rho\eta\phi_{1yt} - \epsilon\eta\phi_{2yt}$$

$$+ \frac{1}{2}\epsilon\rho(\phi_{1x}^2 + \phi_{1y}^2) - \frac{1}{2}\epsilon(\phi_{2x}^2 + \phi_{2y}^2) = O(\epsilon^2) \text{ on } y = 0, \quad (2.1f)$$

$$\phi_{2y} - \xi_t - \epsilon(\xi\phi_{2x})_x = O(\epsilon^2) \text{ on } y = 1-h, \quad (2.1g)$$

$$\phi_{2t} + \xi + \epsilon\xi\phi_{2yt} + \frac{1}{2}\epsilon(\phi_{2x}^2 + \phi_{2y}^2) = O(\epsilon^2) \text{ on } y = 1-h. \quad (2.1h)$$

Spatially periodic solutions are sought of the form

$$\xi = \frac{1}{2} \sum_{k=1}^{\infty} A_k(t) \exp i(k\mu x - \omega_k t) + * , \quad (2.2a)$$

$$\eta = \frac{1}{2} \sum_{k=1}^{\infty} B_k(t) \exp i(k\mu x - \omega_k t) + * , \quad (2.2b)$$

$$\phi_1 = \frac{1}{2} \sum_{k=1}^{\infty} C_{1k}(t) \cosh k\mu(y+h) \exp i(k\mu x - \omega_k t) + * , \quad (2.2c)$$

$$\phi_2 = \frac{1}{2} \sum_{k=1}^{\infty} (C_{2k}(t) \cosh k\mu y + D_{2k}(t) \sinh k\mu y) \exp i(k\mu x - \omega_k t) + * , \quad (2.2d)$$

where * denotes complex conjugate, and k, ω_k are non-dimensional wavenumber (in units of $1/\ell$) and frequency (in units of $(g/h_1 + h_2)^{1/2}$).

Substitution of these Fourier series in equations (2.1) followed by neglect of the $O(\epsilon)$ terms yields the linear approximation, whose solution is (with $T_1 = \tanh k\mu h$, $T_2 = \tanh k\mu(1-h)$)

$$(\rho + T_1 T_2)(\omega_k^2/k\mu)^2 - \rho(T_1 + T_2) \omega_k^2/k\mu + (\rho - 1) T_1 T_2 = 0, \quad (2.3)$$

$$\begin{aligned} B_k &= (1 - T_2 k\mu/\omega_k^2) \cosh \{k\mu(1-h)\} A_k = (ik\mu/\omega_k) \sinh \{k\mu h\} C_{1k} \\ &= (ik\mu/\omega_k) D_{2k} = (ik\mu/\omega_k)(\omega_k^2/k\mu - T_2)/(1 - T_2 \omega_k^2/k\mu) C_{2k}. \end{aligned} \quad (2.4)$$

Equation (2.3) is the dispersion relation, with the solution

$$\frac{\omega_k^2}{k\mu} = \frac{\rho(T_1 + T_2)}{2(\rho + T_1 T_2)} \left[1 \pm \left(1 - \frac{4(\rho + T_1 T_2)T_1 T_2}{\rho(T_1 + T_2)^2} - \frac{\rho - 1}{\rho} \right)^{1/2} \right], \quad (2.5)$$

where the larger root will be denoted ω_{Ak} , and the smaller root ω_{Bk} . When $\rho = 1 + \Delta\rho$, $\Delta\rho \ll 1$, as in the present application, the two roots reduce to

$$\begin{aligned} \omega_{Ak}^2 &= k\mu \tanh k\mu (1 + O(\Delta\rho)), \\ \omega_{Bk}^2 &= \Delta\rho T_1 T_2 / (T_1 + T_2)(1 + O(\Delta\rho)). \end{aligned}$$

The fast wave mode with frequency ω_{Ak} is the free surface wave mode with properties almost independent of the presence of the interface. The slow wave mode with frequency ω_{Bk} is dependent on the reduced gravity $g\Delta\rho$ at the interface, with a free surface displacement that is small compared with the

interface displacement.

The linear solution in equations (2.3) and (2.4) may now be used in the calculation of the next approximation, that is, in the substitution of equations (2.2) in equations (2.1) including the evaluation of the $O(\epsilon)$ terms. When the velocity potential amplitudes C_{1k} , C_{2k} , D_{2k} are eliminated, two differential equations emerge from lengthy calculation, namely (with $D = d/dt$),

$$\begin{aligned} & D(D - 2i\omega_k)(A_k + (\rho - 1)(1 - T_2 k\mu/\omega_k^2) \cosh \{k\mu(1-h)\} B_k) \\ &= \frac{1}{2}\epsilon \sum_{\ell=1}^{k-1} P_{k,-\ell} B_\ell B_{k-\ell} \exp - i(\omega_\ell + \omega_{k-\ell} - \omega_k)t \\ &+ \epsilon \sum_{\ell=1}^{\infty} P_{k,\ell} B_\ell^* B_{k+\ell} \exp - i(\omega_{k+\ell} - \omega_\ell - \omega_k)t + O(\epsilon^2), \\ & \quad k = 1, 2, \dots, \end{aligned} \quad (2.6a)$$

$$\begin{aligned} & (D - i(\omega_k - \omega_{Ak} \omega_{Bk}/\omega_k))(D - i(\omega_k + \omega_{Ak} \omega_{Bk}/\omega_k))(B_k - \\ & (1 - T_2 k\mu/\omega_k^2) \cosh \{k\mu(1-h)\} A_k) \\ &= \frac{1}{2}\epsilon \sum_{\ell=1}^{k-1} Q_{k,-\ell} B_\ell B_{k-\ell} \exp - i(\omega_\ell + \omega_{k-\ell} - \omega_k)t \\ &+ \epsilon \sum_{\ell=1}^{\infty} Q_{k,\ell} B_\ell^* B_{k+\ell} \exp - i(\omega_{k+\ell} - \omega_\ell - \omega_k)t + O(\epsilon^2), \\ & \quad k = 1, 2, \dots. \end{aligned} \quad (2.6b)$$

The frequencies ω_ℓ defined for positive wavenumbers by equation (2.5) are continued to negative wavenumbers by $\omega_{-\ell} = -\omega_\ell$ ($\ell > 0$). The coefficients $P_{k,\ell}$, $Q_{k,\ell}$ are stated in the Appendix. Note that $P_{k,-\ell} = P_{k,-(k-\ell)}$, $Q_{k,-\ell} = Q_{k,-(k-\ell)}$, $0 < \ell < k$.

Equation (2.6a) has a complementary function which when substituted into equations (2.2a) or (2.2b) yields wave harmonics with exponents $k\mu x \pm \omega_k t$. For a given initial displacement, this equation describes waves of one mode (either fast or slow) propagating in the positive and negative x-directions, modified as they propagate by the nonlinear right hand side. The complementary function of equation (2.6b), when substituted

into equations (2.2a) or (2.2b), yields wave modes with exponents $k\mu x \pm \omega_{Ak} \omega_{Bk} / \omega_k t$. The frequency ω_k is equal either to ω_{Ak} for a fast mode or ω_{Bk} for a slow mode. Hence, for a given initial displacement, equation (2.6b) describes waves of the mode other than that in equation (2.6a) propagating in the positive and negative x-directions.

If equation (2.6a) is integrated as it stands, the right hand side of the resulting equation would contain the denominators $-i(\omega_\ell + \omega_{k-\ell} - \omega_k)$ and $-i(\omega_{k+\ell} - \omega_\ell - \omega_k)$. When all three frequencies in either of these denominators are of the slow mode, the expressions are $O(\mu^2)$ as $\mu \rightarrow 0$ (equation 1.1). Since the equations will be applied to long/waves for which $\epsilon/\mu^2 = O(1)$, this integration is not permissible. When equation (2.6a) is multiplied by $\exp(-2i\omega_k t)$, no such difficulty occurs and the equation integrates to

$$\begin{aligned} & D(A_k + (\rho - 1)(1 - T_2 k\mu/\omega_k^2) \cosh \{k\mu(1-h)\} B_k) \\ &= \frac{1}{2} i \epsilon \sum_{\ell=1}^{k-1} \frac{P_{k,-\ell}}{\omega_\ell + \omega_{k-\ell} + \omega_k} B_\ell B_{k-\ell} \exp -i(\omega_\ell + \omega_{k-\ell} - \omega_k)t \\ &+ i \epsilon \sum_{\ell=1}^{\infty} \frac{P_{k,\ell}}{\omega_{k+\ell} - \omega_\ell + \omega_k} B_\ell^* B_{k+\ell} \exp -i(\omega_{k+\ell} - \omega_\ell - \omega_k)t \\ &+ O(\epsilon^2), k = 1, 2, \dots \end{aligned} \quad (2.7a)$$

When equation (2.6b) is multiplied by the integrating factor $\exp -i(\omega_k + \omega_{Ak} \omega_{Bk} / \omega_k)t$ and integrated, it becomes

$$\begin{aligned} & (D - i(\omega_k - \omega_{Ak} \omega_{Bk} / \omega_k))(B_k - (1 - T_2 k\mu/\omega_k^2) \cosh \{k\mu(1-h)\} A_k) \\ &= \frac{1}{2} i \epsilon \sum_{\ell=1}^{k-1} \frac{Q_{k,-\ell}}{\omega_\ell + \omega_{k-\ell} + \omega_{Ak} \omega_{Bk} / \omega_k} B_\ell B_{k-\ell} \exp -i(\omega_\ell + \omega_{k-\ell} - \omega_k)t \\ &+ i \epsilon \sum_{\ell=1}^{\infty} \frac{Q_{k,\ell}}{\omega_{k+\ell} - \omega_\ell + \omega_{Ak} \omega_{Bk} / \omega_k} B_\ell^* B_{k+\ell} \exp -i(\omega_{k+\ell} - \omega_\ell - \omega_k)t \\ &+ O(\epsilon^2), k = 1, 2, \dots \end{aligned} \quad (2.7b)$$

If this equation is now multiplied by the integrating factor $\exp -i(\omega_k - \omega_{Ak} \omega_{Bk} / \omega_k)t$ and integrated, the right hand side of the resulting equation contains the denominators $-i(\omega_\ell + \omega_{k-\ell} - \omega_{Ak} \omega_{Bk} / \omega_k)$ and $-i(\omega_{k+\ell} - \omega_\ell - \omega_{Ak} \omega_{Bk} / \omega_k)$. Either or both of these denominators may have a

magnitude small compared with 1 when k and ℓ are such that the triad describes the near-resonant interaction of equation (1.2). If attention is restricted to those k and ℓ for which these denominators have a magnitude comparable with 1, equation (2.7b) may be multiplied by the integrating factor and integrated to leave

$$\begin{aligned}
 B_k &= (1 - T_2 k\mu/\omega_k^2) \cosh \{k\mu(1-h)\} A_k \\
 &= -\frac{1}{2}\epsilon \sum_{\ell=1}^{k-1} \frac{Q_{k,-\ell}}{(\omega_\ell + \omega_{k-\ell})^2 - (\omega_{Ak} \omega_{Bk}/\omega_k)^2} B_\ell B_{k-\ell} \exp -i(\omega_\ell + \omega_{k-\ell} - \omega_k)t \\
 &\quad - \epsilon \sum_{\ell=1}^{\infty} \frac{Q_{k,\ell}}{(\omega_{k+\ell} - \omega_\ell)^2 - (\omega_{Ak} \omega_{Bk}/\omega_k)^2} B_\ell^* B_{k+\ell} \exp -i(\omega_{k+\ell} - \omega_\ell - \omega_k)t \\
 &\quad + O(\epsilon^2), \quad k = 1, 2, \dots \quad (2.8)
 \end{aligned}$$

Benney [8] derived equations for the time evolution of long nonlinear waves, that is, waves for which $\mu^2 \sim \epsilon \ll 1$. His analysis, applied to the present problem, predicts that for a long nonlinear wave on the free surface ξ satisfies a Korteweg and de Vries equation, while for a long nonlinear wave on the interface η satisfies a Korteweg and de Vries equation. The latter equation is now derived by taking the long wave limits of equations (2.7a) and (2.8) with ω_k , ω_ℓ , $\omega_{k-\ell}$ and $\omega_{k+\ell}$ all referring to the slow interface wave mode.

The linear long wave velocity on the interface is

$$C_0 = \lim_{\mu \rightarrow 0} \omega_{Bk}/k\mu,$$

and, from equation (2.3), is the smaller positive root of

$$C_0^4 - C_0^2 + h(1-h)(\rho-1)/\rho = 0. \quad (2.9)$$

The coefficients $P_{k,\ell}/(\omega_{k+\ell} - \omega_\ell + \omega_k)$ in equation (2.7a) reduce to

$$-\frac{3\rho C_0 k\mu}{4h^2} \frac{C_0^4 + (3h-2)C_0^2 + 1 - 2h}{C_0^2 - (1-h)} (1 + O(\mu^2))$$

and the coefficients $Q_{k,\ell}$ in equation (2.8) are $O(\mu^2)$. On substitution from equation (2.8), equation (2.7a) reduces to

$$\begin{aligned}
DB_k = & -\frac{1}{2}i\epsilon r \sum_{\ell=1}^{k-1} k\mu B_\ell B_{k-\ell} \exp -i(\omega_\ell + \omega_{k-\ell} - \omega_k) t \\
& - i\epsilon r \sum_{\ell=1}^{\infty} k\mu B_\ell^* B_{k+\ell} \exp -i(\omega_{k+\ell} - \omega_\ell - \omega_k) t \\
& + O(\epsilon^2), \quad k = 1, 2, \dots, \quad (2.10)
\end{aligned}$$

$$\text{where } r = \frac{3C_0}{4h} \frac{C_0^4 + (3h-2)C_0^2 + 1 - 2h}{(2C_0^2 - 1)(C_0^2 - (1-h))} (1 + O(\mu^2)).$$

Equation (2.10) may be summed over ℓ and k , using equation (2.2b), to give

$$\eta_t + C_0 \eta_x + 2\epsilon r \eta \eta_x + \mu^2 s \eta_{xxx} = 0 \quad (\epsilon^2, \epsilon\mu^2, \mu^4), \quad (2.11)$$

where, from equation (2.3),

$$\begin{aligned}
\omega_k/k\mu &= C_0 - k^2\mu^2 s + O(\mu^4), \\
\text{and } s &= \frac{C_0}{6} \frac{(1 + (3/\rho - 2)h(1-h))C_0^2 - h(1-h)}{2C_0^2 - 1}.
\end{aligned}$$

Equation (2.11) is a Korteweg and de Vries equation, as predicted by Benney [8].

3. Permanent waves on the interface

Permanent periodic waves of (nondimensional) velocity c on the interface have the Fourier expansion

$$\eta(x, t) = \sum_{k=1}^{\infty} b_k \cos k\mu(x - ct), \quad (3.1)$$

where from equation (2.2b)

$$B_k(t) = b_k \exp i(\omega_k - k\mu c) t. \quad (3.2)$$

When A_k is eliminated between equations (2.7a) and (2.8), and B_k is replaced from equation (3.2), then

$$\begin{aligned}
(\omega_k - k\mu c)b_k &= \frac{1}{2}\epsilon \sum_{\ell=1}^{k-1} R_{k,-\ell} b_\ell b_{k-\ell} + \epsilon \sum_{\ell=1}^{\infty} R_{k,\ell} b_\ell b_{k+\ell} \\
&+ O(\epsilon^2), \quad k = 1, 2, \dots, \quad (3.3)
\end{aligned}$$

where the coefficients $R_{k,\ell}$ are given in terms of $P_{k,\ell}$, $Q_{k,\ell}$ in the Appendix.

If the wave height, trough to crest, is denoted by $2b$, where

$\epsilon = b/(h_1 + h_2)$, then

$$\sum_{k=1}^{\infty} b_{2k-1} = -1 \quad (3.4)$$

where the origin in $x - ct$ is taken at the trough of the wave.

The properties and method of solution of equations (3.3) have been described previously [6] for permanent waves on a single layer fluid, and apply again here. For waves of length small or comparable with the lesser of the layer depths, the permanent waves are Stokes' waves on the interface for which $b_1 = -1$, $b_2 = O(\epsilon)$. For longer waves, as μ decreases, the nonlinear interactions between the wave harmonics lie closer to resonance, and the permanent waves therefore contain more harmonics. Starting from large values of μ , equations (3.3) may be solved numerically for successively smaller values of μ to any required numerical accuracy, with the neglect of the $O(\epsilon^2)$ remainder. One wavelength of the solution for $\rho = 1.05$, $h = 0.9$, $\epsilon = 0.05$, and $\mu = 2$ is sketched in figure 1. This periodic permanent wave is closely approximated by the cnoidal wave solutions of the Korteweg and de Vries equation (2.11), since for a small upper layer ($h = 0.9$), the coefficients r and s in equation (2.11) are of comparable magnitude when $(1-h)^2\mu^2 \sim \epsilon$. As equations (3.3) are solved for smaller values of μ at constant ρ , h , and ϵ , the solutions tend towards periodically spaced solitary waves, and the number of harmonics increases. The solution in figure 1 for $\mu = 2$ contains 11 harmonics exceeding 10^{-3} in magnitude, while that for $\mu = 0.2$ contains 71 harmonics exceeding 10^{-3} in magnitude.

The present calculations have been checked analytically against two previous investigations of the long wave limit. Long permanent waves at the interface of a two layer fluid were investigated by Peters & Stoker [7], who developed perturbation expansions for the streamline displacements in the corresponding steady flow problem. Their solutions agree exactly with the cnoidal and solitary wave solutions of equation (2.11). Benjamin [9] showed that long permanent wave solutions exist for a wide class of fluids whose

density and velocity are arbitrary functions of height. When his method is applied to the particular case of a two layer open fluid, agreement is obtained again with the cnoidal and solitary wave solutions of equation (2.11).

The coefficient r in equation (2.11) is negative when the interface is high, positive when the interface is low, and $r=0$ for $\Delta\rho \ll 1$ when

$$h = \frac{1}{2}(1 - \frac{1}{8} \Delta\rho + O(\Delta\rho)^2). \quad (3.5)$$

When $r < 0$, the cnoidal wave solutions of equation (2.11) are peaked towards the troughs, as in figure 1. As the upper layer is increased in depth and r approaches zero, the periodic solutions tend towards the sinusoidal solution of equation (2.11) for $r = 0$. When $r > 0$, the cnoidal wave solutions of equation (2.11) are peaked towards the crests, as in figure 1 inverted. The same properties are true of the solitary wave solutions of equation (2.11), although as was noticed by Peters and Stoker, there is no solitary wave solution for which $\mu^2 = O(\epsilon)$ when $r = 0$. In this case, following Benney [8], equation (2.11) may be rewritten

$$\eta_t + C_0 \eta_x + 3\epsilon^2 \lambda \eta^2 \eta_x + \mu^2 s \eta_{xxx} = O(\epsilon^3, \epsilon\mu^2, \mu^4), \quad (3.6)$$

where $\mu = O(\epsilon)$ and λ is an $O(1)$ coefficient, and this equation does have solitary wave solutions.

4. Permanent wave structures

Periodic permanent wave structures containing both the fast free surface wave mode and the slow interface wave mode are now investigated. Solutions to the governing equations are sought of the form

$$\eta = \sum_{k=1}^n b_k \cos k\mu(x-ct) \quad , \quad (4.1a)$$

$$\xi = \sum_{k=m_1}^{m_2} a_k \cos \{k\mu(x-ct) - \alpha t\} \quad , \quad (4.1b)$$

where b_k ($1 \leq k \leq n$), a_k ($m_1 \leq k \leq m_2$), c and α are to be determined. The form of these solutions is such that the interface wave and the envelope of the surface wave group are in phase, and the surface wave itself moves

with a constant frequency α relative to the group envelope. The corresponding complex amplitudes, from equations (2.2), are

$$B_k(t) = b_k \exp i(\omega_k - k\mu c)t, \quad 1 \leq k \leq n, \quad (4.2a)$$

$$A_k(t) = a_k \exp i(\omega_k - k\mu c - \alpha)t, \quad m_1 \leq k \leq m_2. \quad (4.2b)$$

The significant nonlinear interactions are divided into three types:

I. Two interface wave modes interacting to modify a third interface wave mode,

$$\omega_{B,k-\ell} + \omega_{B\ell} \approx \omega_{Bk}, \quad 1 \leq |\ell|, k-\ell, k \leq n. \quad (4.3a)$$

Equation (2.8) is valid for this interaction, since $\omega_{B,k-\ell} + \omega_{B\ell} - \omega_{Bk}$ is comparable with 1.

II. Two free surface wave modes interacting to modify an interface wave mode,

$$\omega_{A,k+\ell} - \omega_{A\ell} \approx \omega_{Bk}, \quad 1 \leq k \leq n, \quad m_1 \leq \ell, k+\ell \leq m_2. \quad (4.3b)$$

Equation (2.8) is valid for this interaction also since $\omega_{A,k+\ell} - \omega_{A\ell} - \omega_{Bk}$ is comparable with 1.

III. An interface wave mode and a free surface wave mode interacting to modify a free surface wave mode,

$$\omega_{A,k-\ell} + \omega_{B\ell} \approx \omega_{Ak}, \quad 1 \leq |\ell| \leq n, \quad m_1 \leq k-\ell, k \leq m_2. \quad (4.3c)$$

Equation (2.8) is valid here also because $\omega_{A,k-\ell} + \omega_{B\ell} - \omega_{Ak}$ is comparable with 1.

These three types of quadratic interaction dominate all other nonlinear interactions because of their nearness to resonance. For this reason, they are the only nonlinear interactions included in the calculations.

The governing equations are formulated in terms of the Fourier amplitudes defined in equations (4.2), for otherwise exponentially large coefficients are multiplied by exponentially small amplitudes. The free surface amplitudes A_k ($m_1 \leq k \leq m_2$) have associated with them exponentially small interface amplitudes B_k ($m_1 \leq k \leq m_2$), so it is possible in principle to use equations (2.7a), (2.8) throughout the calculations. This is not desirable in practice because of the errors caused in the numerical calculations. When equations (2.7a), (2.8) are reformulated with the complex amplitudes replaced from

equations (4.2), the governing equations become

$$(\omega_{Bk} - k\mu c)b_k = \frac{1}{2}\epsilon \sum_{\ell=1}^{k-1} (R_1)_{k,-\ell} b_\ell b_{k-\ell} + \epsilon \sum_{\ell=1}^{n-k} (R_1)_{k,\ell} b_\ell b_{k+\ell} + \epsilon \sum_{\ell=m_1}^{m_2-k} (R_2)_{k,\ell} a_\ell a_{k+\ell}, \quad 1 \leq k \leq n, \quad (4.4a)$$

$$(\omega_{Ak} - k\mu c - \alpha)a_k = \epsilon \sum_{\ell=1}^{\text{Min}(n, k-m_1)} (R_3)_{k,-\ell} b_\ell a_{k-\ell} + \epsilon \sum_{\ell=1}^{\text{Min}(n, m_2-k)} (R_3)_{k,\ell} b_\ell a_{k+\ell}, \quad m_1 \leq k \leq m_2. \quad (4.4b)$$

The coefficients R_1 , R_2 , R_3 associated with the three types of nonlinear interaction are defined in the Appendix.

Equation (3.4) measuring the height of the interface wave is still valid, namely

$$\sum_{k \text{ odd}} b_k = -1. \quad (4.5a)$$

Since the height of the wave group on the free surface is independent of the height of the interface wave, then

$$\sum_{k \text{ odd}} a_k = \lambda, \quad (4.5b)$$

where λ is a prescribed constant. The maximum height of the envelope of the wave group above the mean free surface is denoted by a , where $a/(h_1 + h_2) = \epsilon'$. It is to be noted that if a_k ($m_1 \leq k \leq m_2$) is one solution for the free surface harmonics, then $-a_k$ ($m_1 \leq k \leq m_2$) is another solution with the same envelope. The $n + m_2 - m_1 + 3$ equations (4.4), (4.5) are now solved for the $n + m_2 - m_1 + 3$ variables b_k ($1 \leq k \leq n$), a_k ($m_1 \leq k \leq m_2$), c and α .

5. Permanent wave structures of short wavelength.

The simpler solutions of equations (4.4) and (4.5) include those of short wavelength, when the wave on the interface is almost sinusoidal because the first type of interaction is far from resonance. For a free surface wave group of sufficiently small amplitude, equations (4.4a), (4.5a) are then satisfied by $b_1 = -1$, $b_2 = O(\epsilon)$, $c = \omega_{B1}/\mu$, and equations (4.4b) become

$$(\omega_{Ak} - k\omega_{Bl} - \alpha)a_k + \varepsilon(R_3)_{k,-1} a_{k-1} + \varepsilon(R_3)_{k,1} a_{k+1} = 0,$$

$$m_1 \leq k \leq m_2. \quad (5.1)$$

This set of $m_2 - m_1 + 1$ linear algebraic equations has in general $m_2 - m_1 + 1$ sets of solutions, each set containing an eigenvalue α and the corresponding eigenvector a_k ($m_1 \leq k \leq m_2$) of the matrix of coefficients. Each eigenvector may be scaled to satisfy equation (4.5b).

It is a straightforward numerical calculation [10] to find the eigenvalues and eigenvectors of the set of equations (5.1) for any given external parameters. These parameters were taken to be $\rho = 1.05$, $h = 0.9$, $\mu = 20$, $\varepsilon = \varepsilon' = 0.005$, for which the equality $\omega_{Bl} = d\omega_{Ak}/dk$ occurs at about $k = 10.5$. The interval $m_1 \leq k \leq m_2$ was chosen to be sufficiently large that sets of solutions were reproducible to within the desired numerical accuracy (10^{-4}) when the size of the interval was increased further. Each set of solutions was then used as the starting estimate for a Newton-Raphson solution of equations (4.4) and (4.5) to the same numerical accuracy. The first five sets of solutions are drawn in figure 2(a), and the corresponding free surface wave groups (equation 4.1b) are drawn in figure 2(b).

In order to understand the sets of solutions in figure 2(a), equations (5.1) are written as the set of difference equations

$$a_{k+1} - 2a_k + a_{k-1} + f(k) a_k = 0, \quad m_1 \leq k \leq m_2, \quad (5.2)$$

where $(R_3)_{k,-1} \approx (R_3)_{k,1}$, and $f(k)$ is approximately a quadratic form in $k^{-1/2}$.

A comparison of these difference equations with the differential equation

$$\frac{d^2 y}{dx^2} + f(x)y = 0,$$

shows that solutions for a_k are oscillatory in k when $f(k) > 0$, and are convergent or divergent in k when $f(k) < 0$. The only stationary value of $f(k)$ makes it a maximum near $\frac{d}{dk} (\omega_{Ak} - k\omega_{Bl} - \alpha) = 0$, that is, near $\omega_{Bl} = d\omega_{Ak}/dk$. Hence acceptable solutions for a_k ($m_1 \leq k \leq m_2$) consist of a range in the neighbourhood of resonance where a_k is an oscillatory function of k , enclosed by ranges at each end where a_k decreases monotonically in magnitude towards zero. Further, as α decreases, $f(k)$ increases, which means that the extent

of the range of oscillation and the number of oscillations of a_k as a function of k both increase when α decreases. These properties are all present in the five solutions sketched in figure 2(a).

The structures of the free surface wave groups in figure 2(b) may be interpreted in terms of their interaction with the horizontal velocity field caused at the free surface by the wave on the interface. Since the wave on the interface is sinusoidal, the horizontal velocity u at the free surface is also sinusoidal with a positive maximum at the centre of the group and a negative minimum at the two ends of the group. The resonance equation (1.2) is modified now to

$$c = c_g(k) + u, \quad (5.3)$$

where $c = 0.035$ and $-0.001 \leq u \leq 0.001$ (from equations 2.2d, 2.4) for the wave groups in figure 2(b). Hence the wavenumber of the free surface wave within the group varies from 10.8 at the centre of the group to 9.6 where the group extends to the ends of the fundamental wavelength. Measurements in figure 2(b) confirm the accuracy of this interpretation.

6. Permanent wave structures of long wavelength.

When the fundamental wavelength increases, the first type of interaction, namely that between harmonics on the interface, moves closer to resonance. The number of interface harmonics therefore increases, and since each interface harmonic interacts near resonance with a range of pairs of free surface harmonics, the number of free surface harmonics also increases. The latter effect may be seen alternatively as a consequence of a longer interface wave causing a stronger horizontal velocity gradient at the free surface.

Two methods have been developed for calculating numerically the solutions of equations (4.4), (4.5) for long wavelengths. The harmonics of a permanent interface wave of given wavelength in the absence of a free surface wave group, b_k ($1 \leq k \leq n$), may be calculated as in §3 and then substituted into equations (4.4b). The resulting linear algebraic equations for a_k ($m_1 \leq k \leq m_2$) and α may then be solved as in §5 for a free surface wave group of small amplitude,

and the solution used as a starting estimate for a Newton-Raphson solution of equations (4.4), (4.5) at the given wavelength. Alternatively, the solutions in §5 at short wavelengths may be continued step by step in μ to long wavelengths, using the Newton-Raphson method of solution at each step.

The first two sets of solutions for the harmonics at $\rho = 1.05$, $h = 0.9$, $\mu = 2$, $\epsilon = \epsilon' = 0.01$ are shown in figure 3(a), and the corresponding permanent wave structures are sketched in figure 3(b). It can be seen that the shape of the spectra of the free surface harmonics in figure 3(a) is the same as that of the first two forms in figure 2(a). This similarity of shape was found for all five forms in figure 2(a) as μ decreased from 20 to 2. The free surface wave groups in all five forms of permanent wave structure also retained similarity of shape as μ decreased.

The horizontal velocity at the centre of the free surface wave group is 0.008, 0.009 respectively in the two examples in figure 3(b), and the phase velocity is 0.066, 0.067 respectively. Equation (5.3) therefore predicts that the wavenumber at the centre of the free surface group should be about 37 in both examples. The validity of this interpretation is confirmed by figure 3(a), where $k = 37$ lies near the centre of the spectrum in both examples, and by figure 3(b), where measurement of the wavelength within the free surface wave group agrees with this estimate.

The interface wave spectrum is broader in the presence of a wave group than in its absence. The interface spectrum for the first form of permanent wave structure in figure 3 contains 15 harmonics exceeding 10^{-3} in magnitude, while the interface permanent wave spectrum in the absence of a surface wave group contains only 6 harmonics exceeding 10^{-3} in magnitude. The free surface wave group, through the second type of nonlinear interaction identified in §4, broadens the interface wave spectrum and hence sharpens the interface wave.

The amplitude of the free surface wave group (measured by ϵ') may be increased step by step so that the second type of nonlinear interaction causes a greater change to the shape of the wave on the interface. One such example is illustrated in figure 4, which shows the second form of permanent wave

structure at $\rho = 1.05$, $h = 0.9$, $\mu = 2$, $\epsilon = 0.01$, $\epsilon' = 0.05$.

The spectrum of the free surface harmonics in figure 4(a) displays the characteristic shape of the second form of permanent wave structure, but the spectrum of the interface harmonics, instead of decreasing monotonically in magnitude as previously, now displays a small overshoot. It can be seen in figure 4(b) that the shape of the envelope of the free surface wave group has been impressed onto the interface wave, which is a property that also occurs for the other forms of permanent wave structure in this limit. The phase velocity of the structure has increased from 0.067 at $\epsilon = \epsilon' = 0.01$ to 0.124 at $\epsilon = 0.01$, $\epsilon' = 0.05$ because the structure is now dominated by the fast free surface wave mode. The horizontal velocity at the centre of the free surface wave group due to the interface wave is now 0.010, so equation (5.3) predicts that the wavenumber at the centre of the free surface wave group should be about 10. This is in agreement with figures 4(a) and 4(b). The wavenumber is smaller than in the examples of figure 3 because the phase velocity of the structure is larger, requiring from equation (5.3) a larger free surface group velocity.

The amplitude of the interface wave (measured by ϵ) in the examples of figure 3 may be increased step by step while the amplitude of the free surface wave group is held constant. Figure 5 shows the first form of permanent wave structure at $\rho = 1.05$, $h = 0.9$, $\mu = 2$, $\epsilon = 0.05$, $\epsilon' = 0.01$. The phase velocity of the structure is 0.074, which is the same (to this accuracy) as the phase velocity of the permanent interface wave in the absence of a free surface wave group. The horizontal velocity at the centre of the free surface wave group due to the interface wave is 0.045, and from equation (5.3) the wavenumber at the centre of the free surface wave group is therefore about 150. This is consistent with figures 5(a) and 5(b). The central wavenumber is much larger than in the examples of figure 3 because the horizontal velocity at the free surface is much larger, requiring a smaller group velocity in equation (5.3).

When the fundamental wavelength is increased while all other parameters are held constant, the periodic permanent wave structure tends towards a train

of solitary permanent wave structures. The central quarter of one wavelength of the first form of permanent wave structure at $\rho = 1.05$, $h = 0.9$, $\mu = 0.5$, $\epsilon = \epsilon' = 0.01$ is drawn in figure 6(b). The remainder of the wavelength consists of a level free surface and a level interface. The spectra of harmonics of the interface and free surface waves are drawn in figure 6(a) as continuous curves for convenience and because they approximate to the Fourier transforms of a solitary permanent wave structure.

In all the calculations above, the depth of the lower layer is fixed at 0.9 of the total depth ($h = 0.9$). As this ratio is decreased with all other parameters held constant, the horizontal velocity field at the free surface due to the interface wave also decreases, since the interface moves further from the free surface. Beginning from the example of figure 3, as h is decreased at constant ρ , μ , ϵ , and ϵ' , the spectra of the interface wave and free surface wave tend towards those of the example in figure 2. The number of harmonics in the interface wave decreases as h decreases until about $h = 0.35$, when the second harmonic passes through zero. When h is decreased further, the number of harmonics in the interface wave increases again, but the number of harmonics in the free surface wave remains small because the horizontal velocity field at the free surface is also small.

7. Discussion

The permanent wave structures described here consist of a wave of permanent shape at the interface and a wave group of permanent envelope at the free surface. An interface wave has permanent shape when the linear dispersion and the nonlinear steepening or flattening of inclined surfaces is in balance ([9], §1). There is a similar explanation for the permanent shape of the free surface wave envelope. The horizontal velocity field at the free surface due to the interface wave has a forward maximum above the wave trough, decreasing on either side of the trough. Hence a free surface wave behind the trough is stretched and therefore moves faster, since the phase velocity is an increasing function of wavelength. On the other hand, a free surface wave ahead of the trough

is compressed and therefore moves slower. The net effect for the free surface waves is one of balance between the linear dispersion and the nonlinear interaction with the interface wave.

This physical argument may be applied also to wave groups of permanent envelope on deep water ([11], §17.8). In this case, there is a balance between linear dispersion and the mean quadratic velocity field caused at the free surface by the wave group itself.

On comparing the different forms of permanent wave structure in figures 2 or 3, for example, it can be seen that the higher the form, the more complex is the shape of the free surface wave group, although the interface wave remains almost unchanged. Hence, when all other parameters are held constant, the energy of the permanent wave structure is expected to be greater, the higher the form of structure. This in turn implies that the higher forms are less stable, and that the first form of permanent wave structure is most likely to occur in practice. A stability analysis will be made to test this argument.

The unsteady solutions of equations (2.7) will also be investigated. The second type of nonlinear interaction identified in §4, for example, generates interface waves whenever there is a spectrum of free surface waves. When the free surface waves are forced by the wind, this interaction provides a near-resonant mechanism for the generation and growth of interface waves. The permanent wave structures described here may in some sense represent an asymptotic state for waves on a two layer fluid.

Acknowledgment.

The author is grateful to Professor David J. Benney for suggesting this investigation, and for early discussions on it.

References

1. D.J. Benney Significant interactions between small and large scale surface waves. *Stud. Appl. Math.* **55**, 93-106 (1976).
2. M.S. Longuet-Higgins & R.W. Stewart Changes in the form of short gravity waves on long waves and tidal currents. *J. Fluid Mech.* **8**, 565-583 (1960).
3. A.E. Gargett & B.A. Hughes On the interaction of surface and internal waves. *J. Fluid Mech.* **52**, 179-191 (1972).
4. John E. Lewis, Bruce M. Lake & Denny R.S. Ko On the interaction of internal waves and surface gravity waves. *J. Fluid Mech.* **63**, 773-800 (1974).
5. P.J. Bryant Periodic waves in shallow water. *J. Fluid Mech.* **59**, 625-644 (1973).
6. P.J. Bryant Stability of periodic waves in shallow water. *J. Fluid Mech.* **66**, 81-96 (1974).
7. A.S. Peters & J.J. Stoker Solitary waves in liquids having non-constant density. *Comm. Pure Appl. Math.* **13**, 115-164 (1960).
8. D.J. Benney Long non-linear waves in fluid flows. *J. Math & Phys.* **45**, 52-63 (1966).
9. T.B. Benjamin Internal waves of finite amplitude and permanent form. *J. Fluid Mech.* **25**, 241-270 (1966).
10. J.H. Wilkinson & C. Reinsch *Linear Algebra*. Springer. (1971).
11. G.B. Whitham *Linear and nonlinear waves*. Wiley. (1974).

Appendix.

Define $F_k = \omega_k^2 \cosh \mu k(1-h) - \mu k \sinh \mu k(1-h)$,

$G_k = \omega_k^2 \sinh \mu k(1-h) - \mu k \cosh \mu k(1-h)$.

Then

$$P_{k,l} = \frac{1}{2} F_k \left[(\rho-1)(\omega_\ell^2 - \omega_\ell \omega_{k+l} + \omega_{k+l}^2) - \frac{\rho(\omega_{k+l} - \omega_\ell)}{\tanh \mu k h} \left(\frac{\omega_{k+l}}{\tanh \mu(k+l)h} + \frac{\omega_\ell}{\tanh \mu \ell h} \right) \right. \\ \left. - \frac{\rho \omega_\ell \omega_{k+l}}{\tanh \mu \ell h \tanh \mu(k+l)h} + \omega_\ell \omega_{k+l} \frac{G_\ell G_{k+l}}{F_\ell F_{k+l}} \right] \\ + \frac{1}{2} G_k (\omega_{k+l} - \omega_\ell) \left(\omega_{k+l} \frac{G_{k+l}}{F_{k+l}} + \omega_\ell \frac{G_\ell}{F_\ell} \right) \\ + \frac{\omega_\ell^2 \omega_{k+l}^2}{2 F_\ell F_{k+l}} \left[\omega_k^2 (\omega_\ell^2 - \omega_\ell \omega_{k+l} + \omega_{k+l}^2 - \frac{\mu^2 \ell(k+l)}{\omega_\ell \omega_{k+l}}) \right. \\ \left. - (\omega_{k+l} - \omega_\ell) \mu^2 k \left(\frac{k+l}{\omega_{k+l}} + \frac{\ell}{\omega_\ell} \right) \right];$$

$$Q_{k,l} = \frac{\mu^2 k^2 \tanh \mu k h \tanh \mu k(1-h)}{2 \omega_k^2 (\rho + \tanh \mu k h \tanh \mu k(1-h))} \left[(\rho-1)(\omega_\ell^2 - \omega_\ell \omega_{k+l} + \omega_{k+l}^2) \right. \\ \left. - \frac{\rho(\omega_{k+l} - \omega_\ell)}{\tanh \mu k h} \left(\frac{\omega_{k+l}}{\tanh \mu(k+l)h} + \frac{\omega_\ell}{\tanh \mu \ell h} \right) \right. \\ \left. - \frac{\rho \omega_\ell \omega_{k+l}}{\tanh \mu \ell h \tanh \mu(k+l)h} + \omega_\ell \omega_{k+l} \frac{G_\ell G_{k+l}}{F_\ell F_{k+l}} \right. \\ \left. + (\omega_{k+l} - \omega_\ell) \left(\frac{\rho}{\tanh \mu k(1-h)} - \frac{(\rho-1)\mu k}{\omega_k^2} \right) \left(\omega_{k+l} \frac{G_{k+l}}{F_{k+l}} + \omega_\ell \frac{G_\ell}{F_\ell} \right) \right. \\ \left. - \frac{(\rho-1)\omega_\ell^2 \omega_{k+l}^2 F_k}{\omega_k^2 F_\ell F_{k+l}} \left(\omega_\ell^2 - \omega_\ell \omega_{k+l} + \omega_{k+l}^2 - \frac{\mu^2 \ell(k+l)}{\omega_\ell \omega_{k+l}} \right) \right] \\ + \frac{\mu^2 k F_k}{2 \omega_k^2} (\omega_{k+l} - \omega_\ell) \left(\frac{k+l}{\omega_{k+l}} + \frac{\ell}{\omega_\ell} \right) \frac{\omega_\ell^2 \omega_{k+l}^2}{F_\ell F_{k+l}};$$

$$R_{k,l} = \left(\frac{\omega_k^2 F_k P_{k,l}}{\omega_{k+l} - \omega_\ell + \omega_k} + \frac{\omega_k^4 (\omega_{k+l} - \omega_\ell - \omega_k) Q_{k,l}}{(\omega_{k+l} - \omega_\ell)^2 - (\omega_{Ak} \omega_{Bk} / \omega_k)^2} \right) / ((\rho-1)F_k^2 + \omega_k^4);$$

$$(R_1)_{k,l} = R_{k,l} \text{ with } \omega_k = \omega_{Bk}, \omega_\ell = \omega_{B\ell}, \omega_{k+l} = \omega_{B,k+l};$$

$$(R_2)_{k,l} = \frac{F_\ell F_{k+l}}{\omega_\ell^2 \omega_{k+l}^2} R_{k,l} \text{ with } \omega_k = \omega_{Bk}, \omega_\ell = \omega_{A\ell}, \omega_{k+l} = \omega_{A,k+l};$$

$$(R_3)_{k,l} = \left(\frac{\omega_k^4 P_{k,l}}{\omega_{k+l} - \omega_l + \omega_k} - \frac{(\rho-1)F_k \omega_k^2 (\omega_{k+l} - \omega_l - \omega_k) Q_{k,l}}{(\omega_{k+l} - \omega_l)^2 (\omega_{Ak} \omega_{Bk} / \omega_k)^2} \right) /$$

$$((\rho-1)F_k^2 + \omega_k^4) \text{ with } \omega_k = \omega_{Ak}, \omega_l = \omega_{Bl}, \omega_{k+l} = \omega_{A,k+l};$$

(Both $(R_2)_{k,l}$ and $(R_3)_{k,l}$ may be approximated by simpler expressions when $k \gg 1$ or $l \gg 1$.)

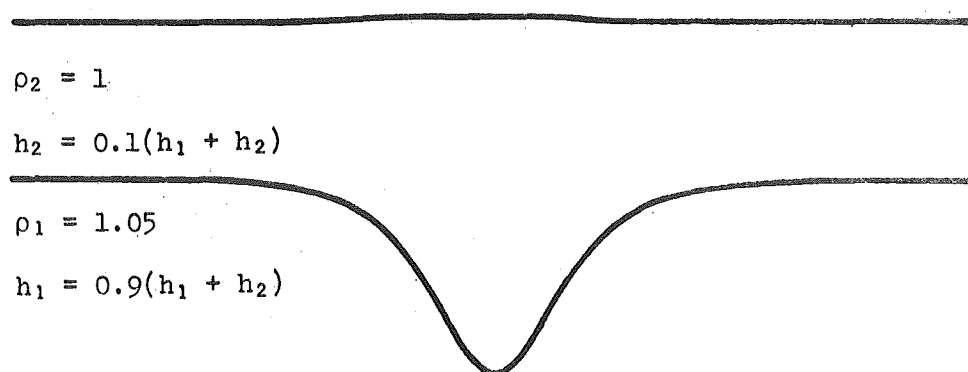


Figure 1. One wavelength of a permanent interface wave (vertical magnification 2π).

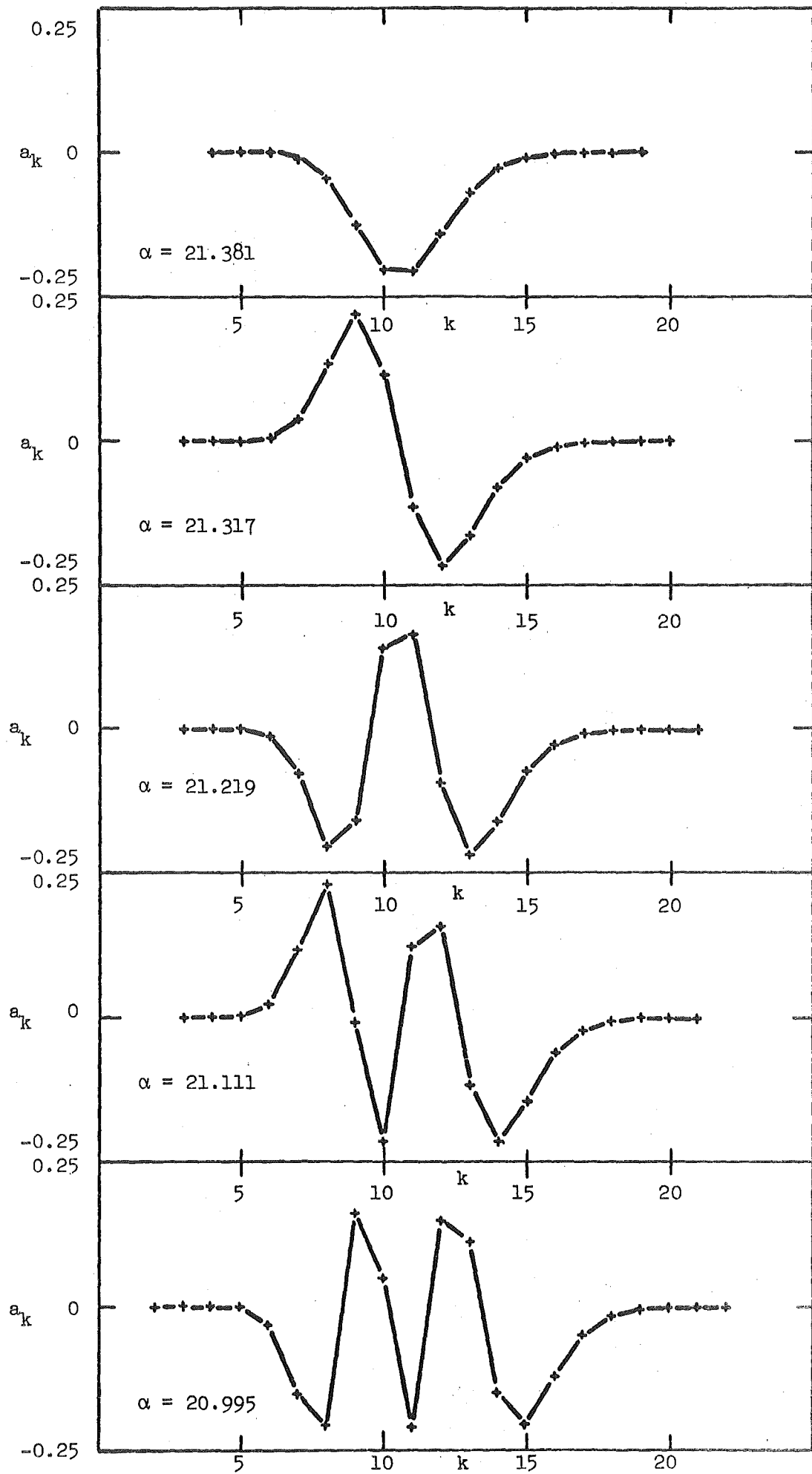


Figure 2(a). Free surface wave spectra for the first five forms of permanent wave structure at short wavelength. The interface harmonics are $b_1 = -1.00$, $|b_2| \sim 0.01$. The points have been joined for clarity.

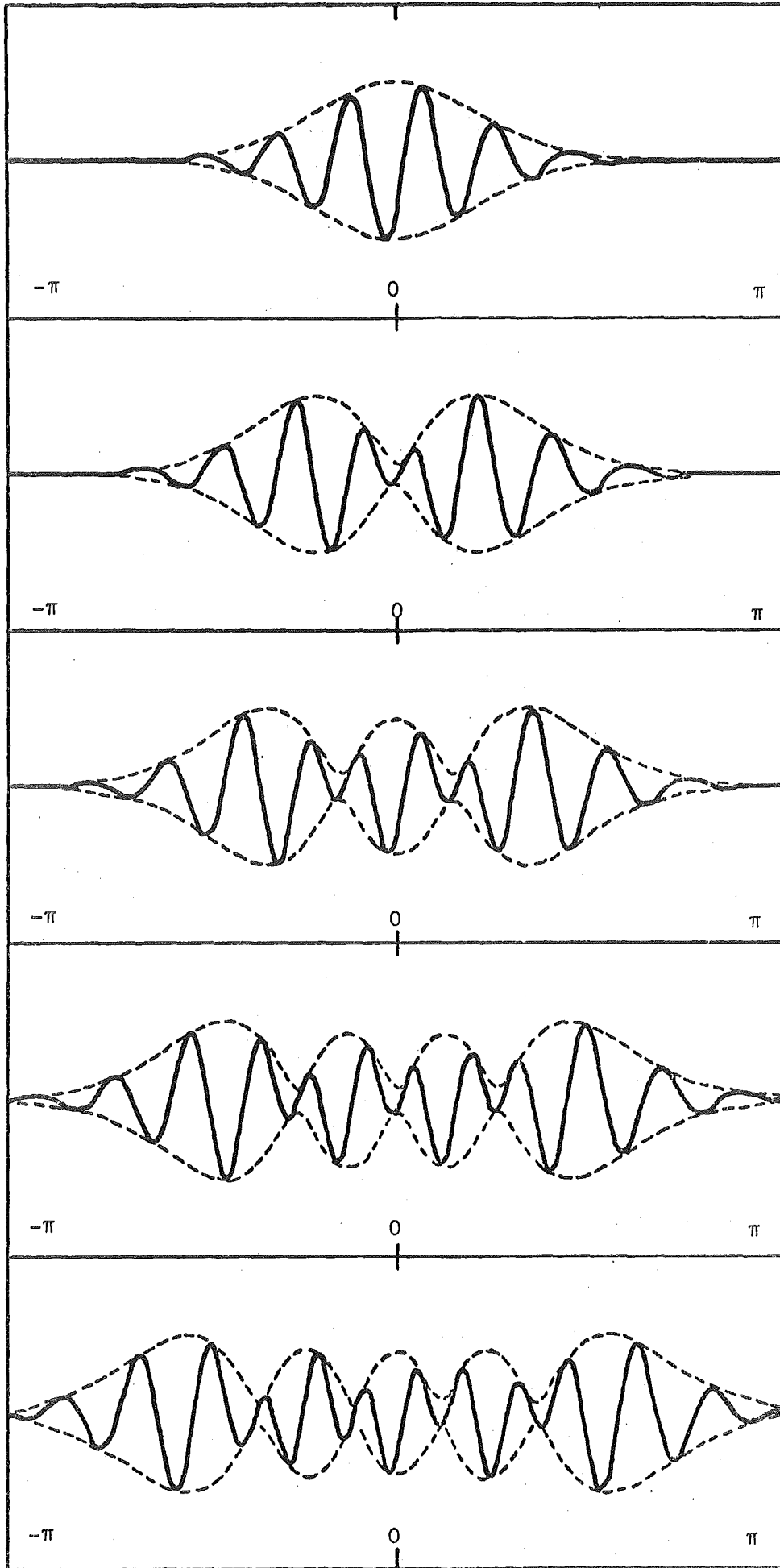


Figure 2(b). One wavelength of the free surface wave groups for the first five forms of permanent wave structure at short wavelength (vertical magnification 2π). The dashed curves show the envelopes of permanent form, and the solid curves the free surface displacement at an instant. The trough of the nearly sinusoidal interface wave lies below the centre of the free surface group.

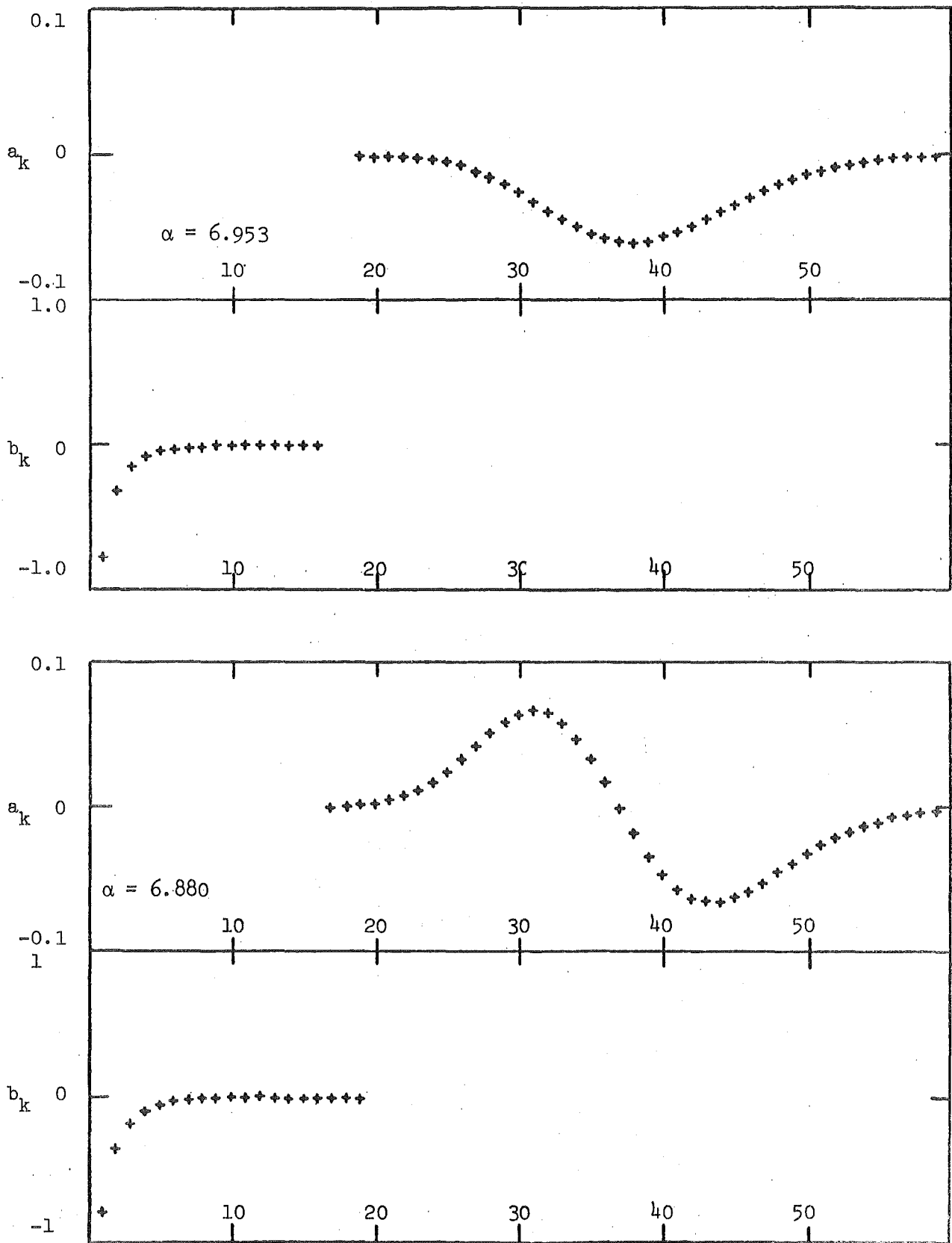


Figure 3(a). Wave spectra for the first two forms of permanent wave structure at long wavelength with $\epsilon = \epsilon' = 0.01$.

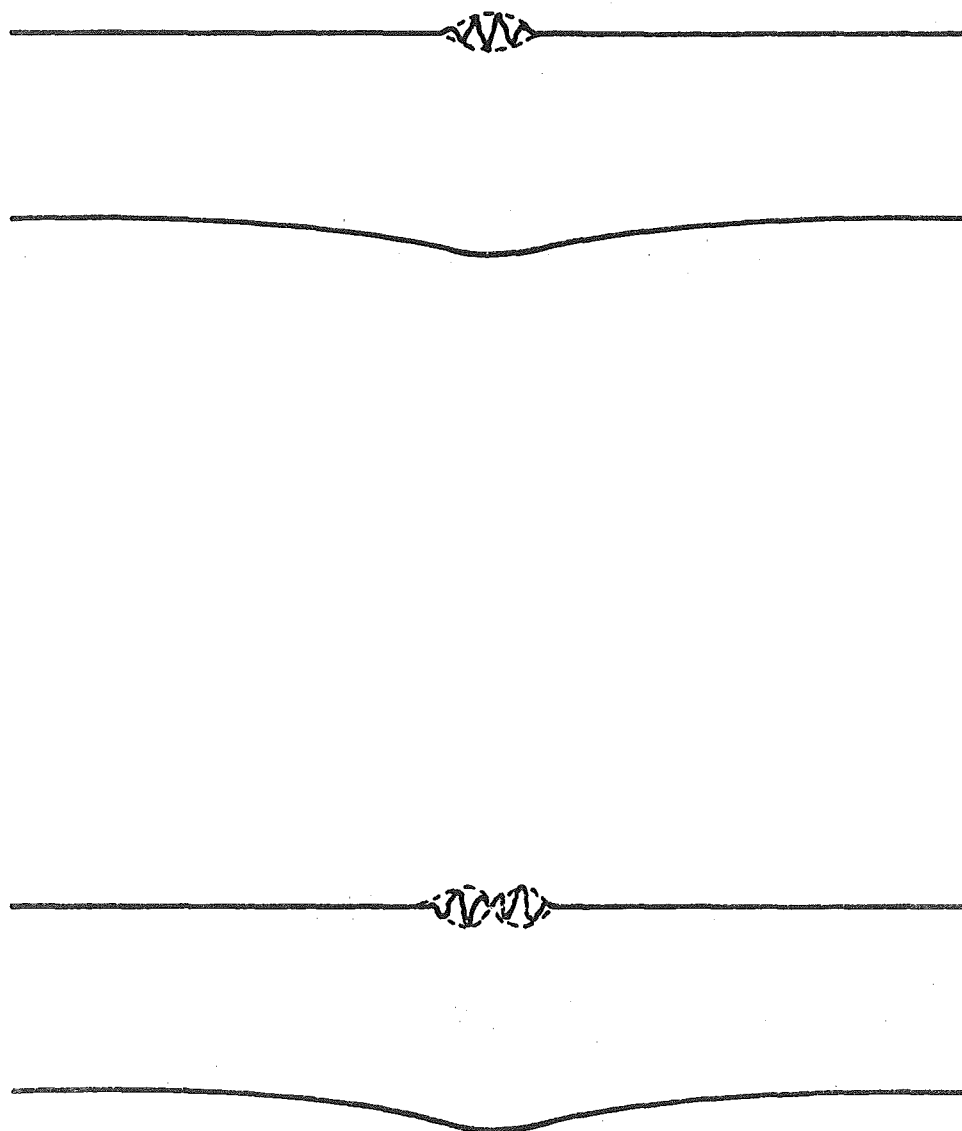


Figure 3(b). One wavelength of the first two forms of permanent wave structure at long wavelength with $\epsilon = \epsilon' = 0.01$ (vertical magnification 2π).

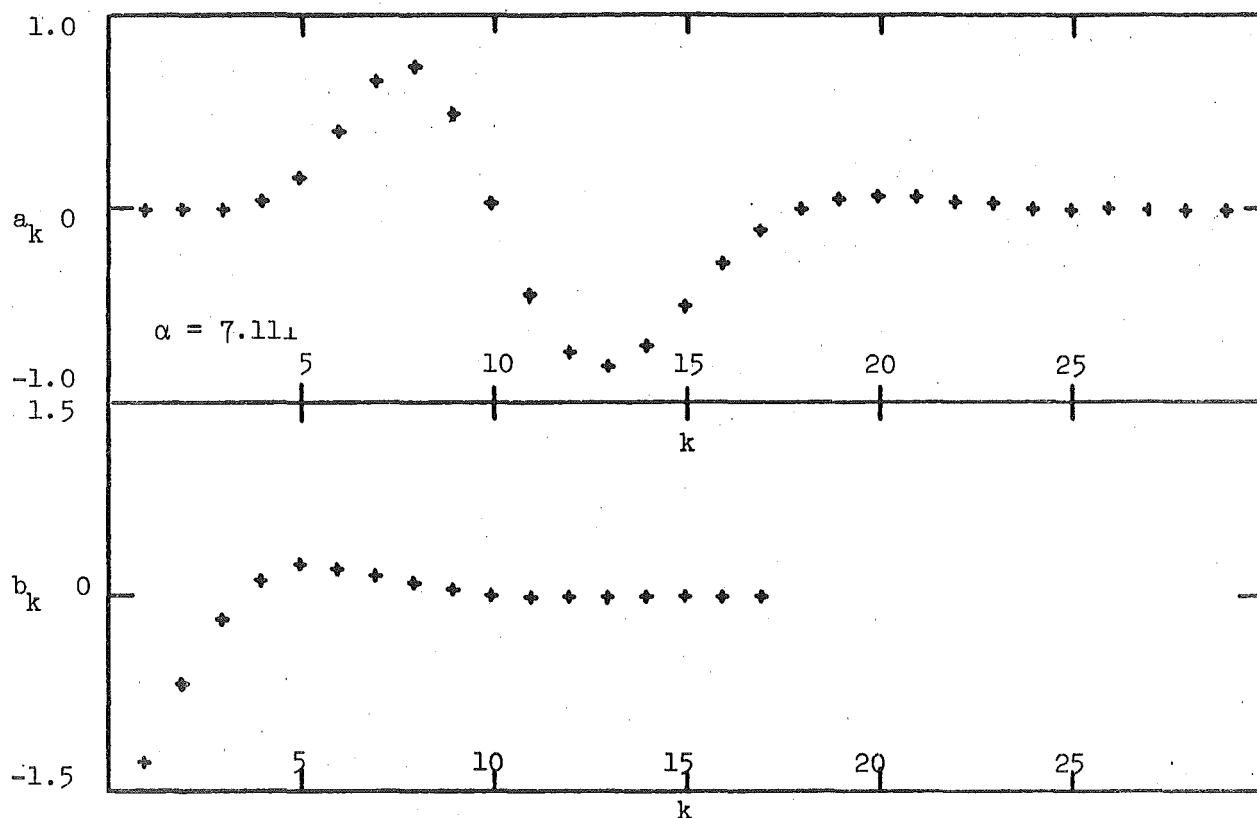


Figure 4(a). Wave spectra for the second form of permanent wave structure at long wavelength with $\epsilon = 0.01$, $\epsilon' = 0.05$.

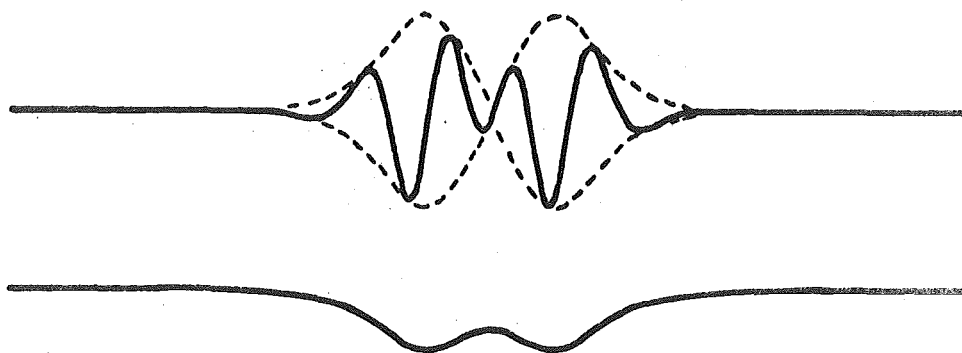


Figure 4(b). One wavelength of the above form of permanent wave structure (vertical magnification 2π).

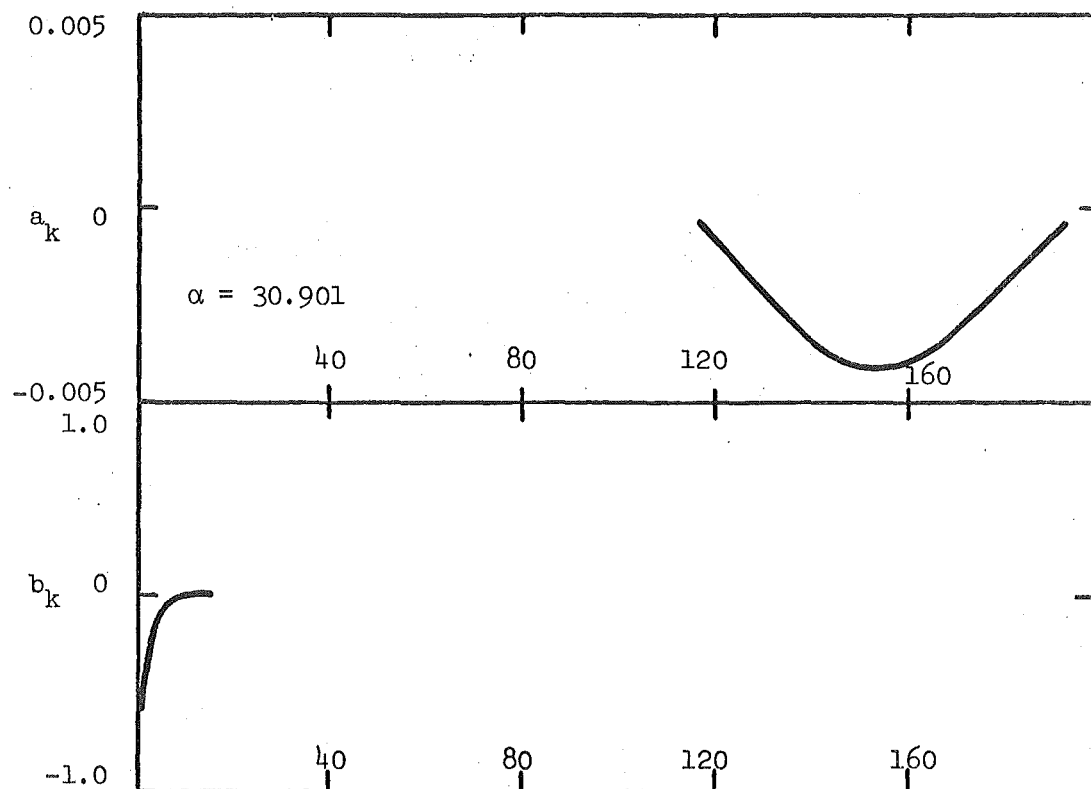


Figure 5(a). Wave spectra for the first form of permanent wave structure at long wavelength with $\varepsilon = 0.05$, $\varepsilon' = 0.01$. The discrete points have been replaced by a continuous curve.

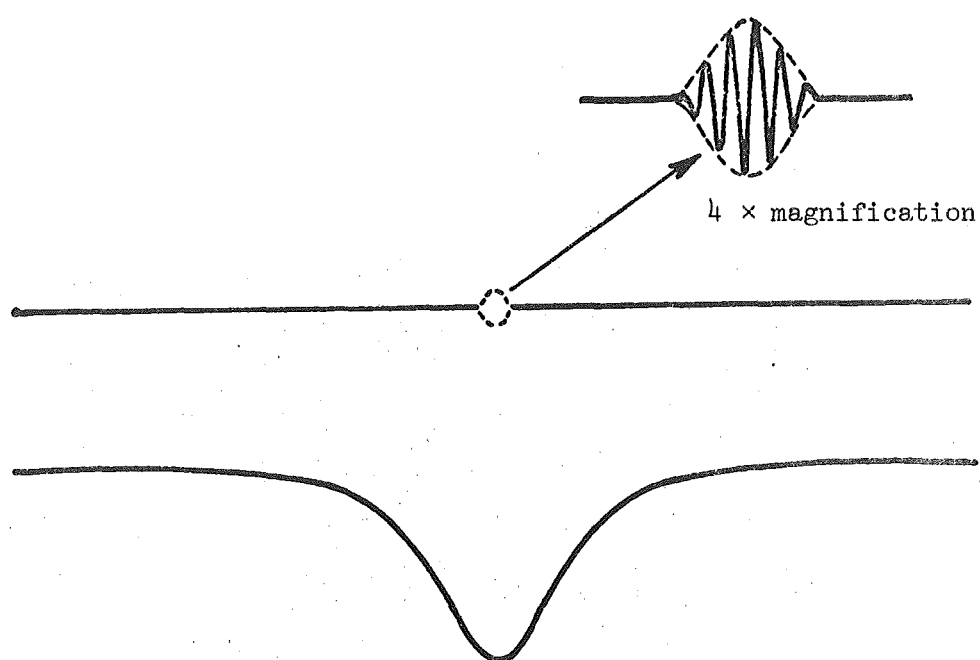


Figure 5(b). One wavelength of the above form of permanent wave structure (vertical magnification 2π).

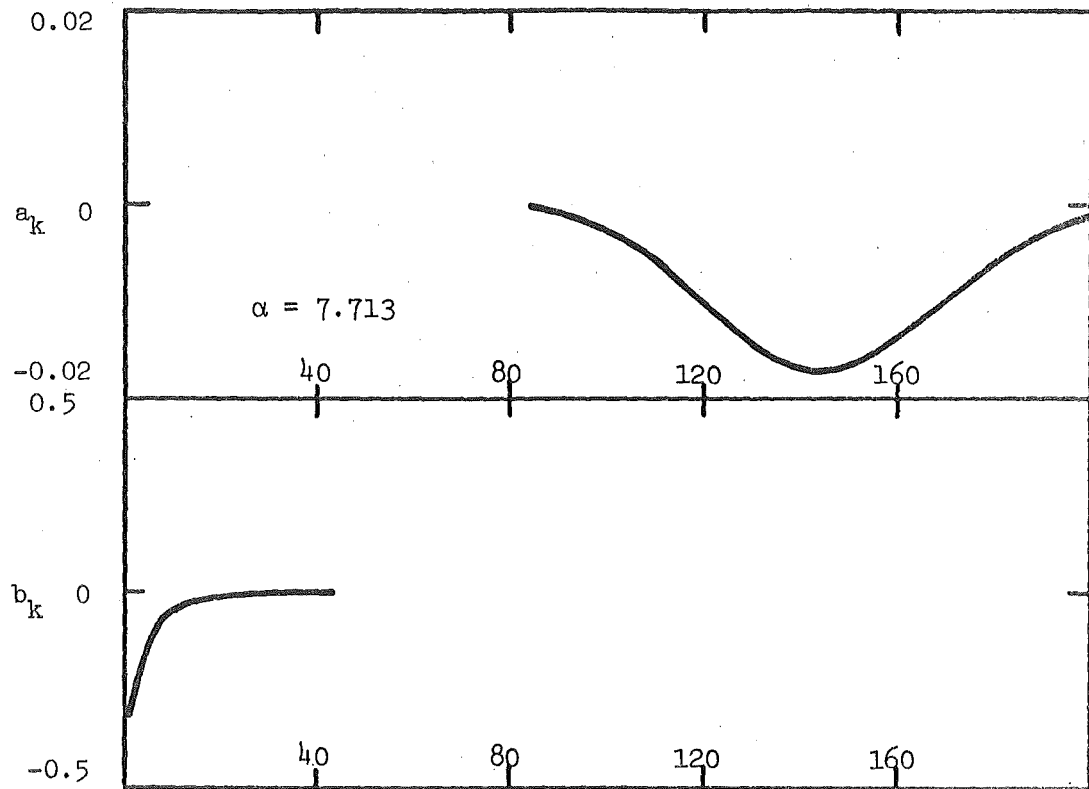


Figure 6(a). Wave spectra for the first form of permanent wave structure at very long wavelength. The discrete points have been replaced by a continuous curve.

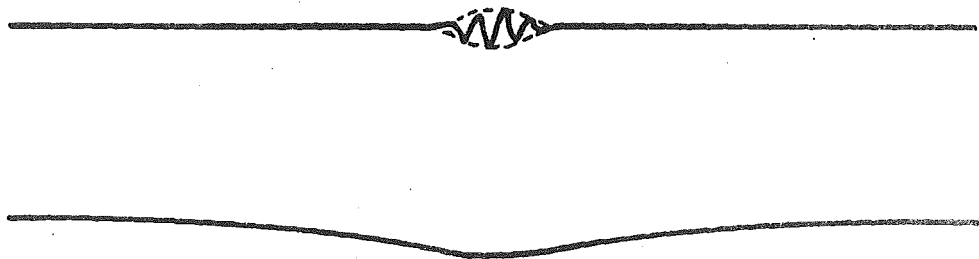


Figure 6(b). The central quarter of one wavelength of the above form of permanent wave structure (vertical magnification 2π).